ORIGINAL ARTICLE

Journal of Cachexia, Sarcopenia and Muscle 2024; **15**: 81–97
Published online 28 November 2023 in Wiley Online Library (wileyonlinelibrary.com) **DOI:** 10.1002/jcsm.13379

Vitamin K1 ameliorates lipopolysaccharide-triggered skeletal muscle damage revealed by faecal bacteria transplantation

Yuru Xiao[1,2], Jianguo Feng[1,2], Jing Jia[1,2], Jie Li[1], Yingshun Zhou[3], Zhangyong Song[4], Fasheng Guan[5], Xuexin Li[5] & Li Liu[1]*

[1]*Department of Anesthesiology, The Affiliated Hospital of Southwest Medical University, Luzhou, China;* [2]*Anesthesiology and Critical Care Medicine Key Laboratory of Luzhou, Southwest Medical University, Luzhou, China;* [3]*Laboratory of Pathogen and Microbiology, Southwest Medical University, Luzhou, China;* [4]*Department of Pathogenic Biology, Southwest Medical University, Luzhou, China;* [5]*Department of Anesthesiology, Southwest Medical University, Luzhou, China*

Abstract

Background Sepsis-associated muscle weakness is common in patients of intensive care units (ICUs), and it is closely associated with poor outcomes. The mechanism of sepsis-induced muscle weakness is unclear. Recent studies have found that gut microbiota and metabolites are involved in the regulation of skeletal muscle mass and metabolism. This study aimed to investigate the effects of gut microbiota and metabolites on sepsis-associated muscle weakness.

Methods In a lipopolysaccharide (LPS)-induced inflammation mouse model, mice with different sensitivities to LPS-induced inflammation were considered as donor mice for the faecal microbiota transplantation (FMT) assay, and recipient mice were divided into sensitive (Sen) and resistant (Res) groups. Skeletal muscle mass and function, as well as colonic barrier integrity were tested and gut microbiota and metabolite composition were analysed in both groups of mice. The effect of intestinal differential metabolite vitamin K1 on LPS-triggered muscle damage was investigated, and the underlying mechanism was explored.

Results Recipients exhibited varying LPS-triggered muscle damage and intestinal barrier disruption. Tibialis anterior (TA) muscle of Sen exhibited upregulated expression levels of MuRF-1 (0.825 ± 0.063 vs. 0.304 ± 0.293, $P = 0.0141$) and MAFbx (1.055 ± 0.079 vs. 0.456 ± 0.3, $P = 0.0092$). Colonic tight junction proteins ZO-1 (0.550 ± 0.087 vs. 0.842 ± 0.094, $P = 0.0492$) and occludin (0.284 ± 0.057 vs. 0.664 ± 0.191, $P = 0.0487$) were significantly downregulated in the Sen group. Metabolomic analysis showed significantly higher vitamin K1 in the faeces ($P = 0.0195$) and serum of the Res group ($P = 0.0079$) than those of the Sen group. After vitamin K1 intervention, muscle atrophy-related protein expression downregulated ($P < 0.05$). Meanwhile SIRT1 protein expression were upregulated (0.320 ± 0.035 vs. 0.685 ± 0.081, $P = 0.0281$) and pNF-κB protein expression were downregulated (0.815 ± 0.295 vs. 0.258 ± 0.130, $P = 0.0308$). PI3K (0.365 ± 0.142 vs. 0.763 ± 0.013, $P = 0.0475$), pAKT (0.493 ± 0.159 vs. 1.183 ± 0.344, $P = 0.0254$) and pmTOR (0.509 ± 0.088 vs. 1.110 ± 0.190, $P = 0.0368$) protein expression levels were upregulated in TA muscle. Meanwhile, vitamin K1 attenuated serum inflammatory factor levels.

Conclusions Vitamin K1 might ameliorate LPS-triggered skeletal muscle damage by antagonizing NF-κB-mediated inflammation through upregulation of SIRT1 and regulating the balance between protein synthesis and catabolism.

Keywords Gut microbiota; Inflammation; Muscle weakness; Sepsis; SIRT1; Vitamin K1

Received: 6 February 2023; Revised: 3 August 2023; Accepted: 25 September 2023
**Correspondence to: Li Liu, Department of Anesthesiology, The Affiliated Hospital of Southwest Medical University, No. 25, Taiping Road, Luzhou, Sichuan 646000, China. Email: niuniudoctor@swmu.edu.cn*

© 2023 The Authors. Journal of Cachexia, Sarcopenia and Muscle published by Wiley Periodicals LLC.
This is an open access article under the terms of the Creative Commons Attribution-NonCommercial-NoDerivs License, which permits use and distribution in any medium, provided the original work is properly cited, the use is non-commercial and no modifications or adaptations are made.

Introduction

Intensive care unit-acquired muscle weakness (ICU-AW) is a common and life-threatening complication in patients with critical illness. It is associated with high morbidity and mortality in ICU.[1] The morbidity of ICU-AW is 30–50% in patients with critical illness and even up to 67% in patients with sepsis. ICU-AW is an independent risk factor for increased mortality in ICU.[2] Sepsis-induced muscle weakness is a common complication of critical illness, it leads to long-term impairment of physical function, and it is associated with loss of function after hospital discharge, prolonged hospital stay, delayed recovery and late death.[3] Abundant studies reported that sepsis enhanced protein degradation and inhibited protein synthesis, which contributed to impaired muscle function and death.[4,5] The pathogenesis is complex and not fully understood.

Many studies recently confirmed that the gut microbiota and metabolites could be involved in sepsis-associated organ dysfunction as regulators of upstream immune activity.[6,7] However, few evidence could be found regarding how the gut microbiota regulates skeletal muscle mass and metabolism function in sepsis, a major metabolic and immune organ in the body. To date, the gut microbiota–muscle axis has been widely proposed. Many in-vitro experiments and preclinical studies showed a close association between muscle and the gut microbiota.[8,9] Elevated microbial taxa of Oscillospira and Ruminococcus and decreased microbial taxa of Barnesiellaceae and Christensenellaceae have been reported to be related with muscle damage.[10] Compared with pathogen-free mice, germ-free mice (lacking gut microbiota) showed reduced skeletal muscle mass and downregulated expression of genes related to skeletal muscle metabolism and function. This finding could be reversed by the application of microbial metabolites.[11] After faecal microbiota transplantation from pig donors, germ-free mice could replicate the skeletal muscle properties, including muscle development and lipogenesis ability.[12] Multiple gut microbial metabolites have been proposed to be involved in skeletal muscle metabolism and inflammation. For instance, Butyrate alleviates muscle atrophy induced by diabetic nephropathy through PI3K/Akt/mTOR signalling.[13] Indole-3-propionic acid (IPA) was found to not only contribute to muscle growth and development, but also have anti-inflammatory effects, partly associated with the IPA/miR-26a-2-3p/IL-1β cascade.[14] Numerous studies showed that the gut microbiota plays an important role in promoting the development of the immune system and maintaining normal immune function.[15] Overall, the gut microbiota is closely related to skeletal muscle content and biochemical and metabolic indicators, and it is the major immune regulator in the gut and extra-gut organs.[16,17] Based on these studies, the gut microbiota and metabolites are possibly key factors in the development of sepsis-induced muscle weakness.

In the present study, the gut microbiota and metabolites were hypothesized to be associated with the development of sepsis-induced muscle weakness. 16sDNA sequencing and metabolic analysis were applied to identify signature differential substances and determine the role and mechanism of protection against lipopolysaccharide-triggered skeletal muscle damage.

Methods

Animals and experimental design

All experiments were performed in accordance with the guidelines of animal experiments and approved by the Animal Ethics Committee of Southwest Medical University (No. 20211122–007). This work confirms to the ethical standards laid down in the 1964 Declaration of Helsinki and its later amendments. Male specific pathogen-free C57BL/6 mice aged 6–8 weeks (20–22 g) were purchased from Beijing Hua Fukang Biotechnology. All animals were domesticated and maintained in the animal facility of Southwest Medical University in a temperature-controlled environment of 21°C–25°C, with a 12-h light/dark cycle and free access to a standard laboratory diet and clean water. Data collection and statistical analysis was conducted blind to group assignment. Mice did not experience unexcepted lethality.

Study 1: 7-day mortality observation experiment

Faeces from C57BL/6J mice (n = 42) were collected before LPS injection. These mice were selected for intraperitoneal injection of lipopolysaccharide (LPS, 10 mg/kg, from *Escherichia coli* O55:B5, Sigma) to screen mice for susceptibility to LPS-induced inflammation. These mice were housed in different cages randomly. If the mice showed a moribund state within 24 h and the severity of sepsis is severe, the mice are sacrificed and defined as the S-sen group. However, the mice that survived for 7 days and recovered to the active state were identified as sepsis resistant mice. These mice were purchased from the same batch.

Study 2: Experiment of faecal microbiota transplantation

Forty mice were randomly divided into four groups by random number table method: (1) healthy control group (Ctrl group, n = 10); (2) antibiotic group (ABX group, n = 10); (3) FMT from S-res group (Res group, n = 10) and (4) FMT from S-sen group (Sen group, n = 10). The Ctrl group was under no treatment. The ABX group was treated daily for 5 days with compound antibiotics by gavage. The Res group was given by gavage daily for 5 days with compound antibiotics and then treated with the faecal lipid of S-res mice, followed by intraperitoneal injection of 15 mg/kg LPS. The Sen group was pretreated daily for 5 days with compound antibiotics by gavage and then treated with the faecal lipid of S-sen

mice, followed by intraperitoneal injection of 15 mg/kg LPS. Mice were sacrificed 24 h after intraperitoneal injection of LPS. Mice were sacrificed and not included in the analysis if they developed a moribund state and the severity of sepsis was severe within 24 h.

Study 3: Experiment of vitamin K1 treatment

Thirty mice were selected and randomly divided into three groups by random number table method: (1) Ctrl group (n = 10), (2) LPS group (n = 10), and (3) vitamin K1 treatment group (VK1 group, n = 10). The Ctrl group was under no treatment. This group of mice is the Ctrl group of mice in study 2. The LPS group was injected intraperitoneally with 15 mg/kg of LPS. The VK1 group was injected intraperitoneally with 15 mg/kg of LPS and then treated with 1 mg/kg BW of vitamin K1 by gavage. Mice were sacrificed 24 h after intraperitoneal injection of LPS.

Faecal microbiota transplantation administration

FMT administration was conducted on the basis of a modified method.[18,19] In a typical procedure, mice received compound antibiotics (100 mg/kg vancomycin, 200 mg/kg neomycin sulphate, 200 mg/kg metronidazole, and 200 mg/kg ampicillin) once daily for 5 days to remove the intrinsic intestinal microbiota. The faeces of each mouse were collected before modelling and resuspended with 1 mL PBS (125 mg:1 mL). The suspension was collected as the transplantation vehicle by vortex vigorously for 1 min and centrifuging at 800 g for 8 min. The faecal bacterial solution was given to the recipient mice by gavage of 150 μL each time, once a day for 3 days.

Sepsis severity score

Sepsis severity was assessed before sacrifice using the following variables: piloerection, alterations in gait, lethargy, alterations in respiratory rate, lacrimation, loss of grip strength, decreased body tone, respiratory difficulty after manipulation, lack of exploratory behaviour, and body temperature alterations, as described previously.[20] Animals received 1 point for each variable presented. The total score reflects the severity of the sepsis. Sepsis severity scores of 2–3 was rated as mild, 4–7 was rated as moderate, and 8–10 was rated as severe. In this study, mice were sacrificed when the severity of sepsis was assessed as severe.

Histopathology

Gastrocnemius (GA) tissues were collected, washed with PBS, fixed with 4% paraformaldehyde solution, dehydrated with ethanol, permeated with xylene, paraffin-embedded, sectioned, and H&E stained. Subsequently, morphological evaluation was performed by light microscopy, and the diameter and cross-sectional area (CSA) of the muscle fibres were recorded to assess the size of the muscle fibres.

Apoptosis detection

Apoptosis of mice GA muscle was detected by TUNEL assay in accordance with the kit instructions. In-vivo paraffin sections were cut to 5 μm thick. TUNEL assay was performed using the TMR (Green) TUNEL Cell Apoptosis Detection Kit (Servicebio, USA), and nuclei were counterstained with DAPI. Positive cells were counted in five different areas of each section and reported as the percentage of TUNEL-positive muscle cells.

Grip strength measurement

Mice were measured for grip strength before sacrifice. The procedure for the tests was as described in a previous study.[21] An experienced researcher made the mice grasp a horizontal metal bar attached to a force sensor and pulled the mouse's tail gently backward. The force sensor automatically recorded the peak tension when the mouse's limbs were released from the horizontal bar. Three grasping-force measurements were performed at each timepoint, and their average values were calculated and recorded. The grasping force was homogenized with body weight.

Electromyographic measurements

After being anaesthetized with pentobarbital sodium, the mice were placed on a heating pad in a prone position. Measurements were performed using an RM6240 system multichannel physiological signal-acquisition and processing system. Compound muscle action potential (CMAP) measurements were typically performed to access hindlimbs nerve functionality. The stimulating electrodes were placed by the side of the sciatic notch, 1 cm apart from each other. The recording electrodes were positioned on the GA muscle subcutaneously, and the reference electrodes were placed on the Achilles tendon. Finally, the ground electrode was placed at the tail. CMAP latency and amplitude were measured. CMAP measurement is a minimally invasive electrophysiologic technique commonly used in clinical and experimental settings to assess neuromuscular nerve conduction. Latency is measured from the stimulation to the start of CMAP response. Amplitude is determined by the maximum negative peak to the maximum positive peak of the bidirectional wave. Latency was used to evaluate the time from nerve signal to muscle stimulus, and amplitude described the number of depolarizing myofibers. The stimulation currents were gradually increased until the amplitude of the CMAP response

reached its maximum value. All measurements were repeated three times. The mice were measured before they were sacrificed.

Serum inflammatory factors detection

After 24 h of modelling, the mice were anaesthetized with sodium pentobarbital, and their eyes were removed for blood sampling and centrifuged at 3000 rpm for 10 min. The supernatant was frozen for examination. The levels of interleukins (IL-1 and IL-6) and TNF-α were measured to assess systemic inflammation by ELISA in accordance with the kit instructions.

Malonic dialdehyde content measurement

GA muscle malonic dialdehyde (MDA) was measured before sacrfice using the lipid peroxidation MDA assay kit (Beyotime). In brief, MDA reacted with thiobarbituric acid (TBA) in higher temperature and acidic environment to form MDA-TBA adducts. These adducts were fluorometrically measured. Their maximum absorption at 535 nm was measured via colorimetric method.

Total superoxide dismutase activity measurement

GA muscle total superoxide dismutase (SOD) activity was measured before sacrfice in accordance with the total superoxide dismutase assay kit with WST-8 (Beyotime, Beijing). In brief, WST-8 reacted with the superoxide anion (O_2^-) catalysed by xanthine oxidase to produce water-soluble formazan dye. SOD could inhibit this reaction step due to its ability to catalyse the disproportionation of superoxide anions. Therefore, SOD activity was negatively correlated with the amount of formazan dye produced, and the enzymatic activity of SOD could be calculated by colorimetric analysis of WST-8 products.

Glutathione reductase measurement

GA muscle glutathione reductase (GR) was reduced to oxidized glutathione to produce reduced glutathione (GSH), and GSH reacted with the substrate DTNB to produce yellow TNB and oxidized glutathione. Then, the level of glutathione reductase activity was calculated by measuring A412.

Western blot analysis

Samples of TA muscle and colonic tissue were collected and extracted. The tissue was homogenized in lysis buffer by using a PRO200 Bio-Gen Senes instrument. Total protein was quantified using a Beyotime BCA protein assay kit, separated by SDS-PAGE in a 10% polyacrylamide gel, and transferred onto nitrocellulose filter membranes. The membranes were then blocked with 5% skimmed milk powder for 2 h at room temperature. Subsequently, the membranes were incubated with primary antibodies at 4°C overnight. After being washed, the membranes were incubated with the corresponding secondary antibodies. Thereafter, the membranes were visualized by ECL chemiluminescence. Finally, they were analysed with ImageJ software. Primary antibodies and dilutions were as follows: Anti-MuRF1 (sc-398606, 1:1000) and anti-MAFbx (sc-166806, 1:1000) from Santa Cruz Biotechnology, USA. Anti-ZO1 (AF5145, 1:1000), anti-occludin (DF7504, 1:1000) and GAPDH (#AF7021) from Affinity, China. Anti-SirT1 (#9475, 1:1000), anti-NF-κB (#8242, 1:1000), anti-phospho-NF-κB (#3033, 1:1000), anti-mTOR (#2983, 1:1000), anti-phospho- mTOR (#5536, 1:1000),anti-AKT (#4691, 1:1000) and anti-phospho-AKT (#4060, 1:1000) from Cell Signaling Technology, USA. Anti-PI3K (AB_10734439) from Proteintech, USA. Secondary antibodies and dilutions were as follows: Goat anti-rabbit lgG antibody (#S0001, 1:20000) and Goat anti-mouse lgG antibody (#43593, 1:20000) from Affinity, China.

16SrDNA sequencing analysis

Fresh faeces were collected after faecal bacterial transplantation. CTAB/SDS method was used to extract the total genome DNA in samples. DNA concentration and purity were monitored on 1% agarose gel. In accordance with the concentration, DNA was diluted to 1 ng/μL with sterile water. The 16SrDNA/18S rDNA/ITS genes in distinct regions were amplified with specific primers and barcodes. Data were analysed using QIIME2 software.

Nontargeted metabolomics

UHPLC–MS/MS analyses were performed using a Vanquish UHPLC system (Thermo Fisher, Germany) coupled with an Orbitrap Q ExactiveTM HF mass spectrometer (Thermo Fisher, Germany). Faeces (100 mg) were individually ground with liquid nitrogen, and the homogenate was resuspended with prechilled 80% methanol by a vortex. The samples were incubated on ice for 5 min and then centrifuged at 15 000 g and 4°C for 20 min. A part of the supernatant was diluted to the final concentration containing 53% methanol by using lipid chromatography-mass spectrometry (LC–MS)-grade water. The samples were subsequently transferred into a fresh Eppendorf tube and then centrifuged at 15 000 g and 4°C for 20 min. Finally, the supernatant was injected into an LC–MS/MS system for analysis.

Targeted metabolomics

Fresh blood was collected from mice in accordance with the method of eye blood sampling and centrifuged at 3000 rpm for 15 min. The supernatant was collected in a 1.5 mL centrifuge tube. The samples were extracted, nitrogen-blown, and re-dissolved with the extracted solution in accordance with the kit instructions [ultra-performance LC-electrospray tandem MS (UPLC-MS/MS)], and then the extracted samples were detected by UPLC-MS/MS on the machine. When the samples first entered the liquid-phase system, they were separated, purified, and concentrated by the column and introduced into the MS system. After ionization in the ion source of the MS system into the triple quadrupole mass analyser, the separation was performed in accordance with the mass-to-charge ratio (m/z) of the ions. Data were collected in multiple reaction monitoring modes, and the chromatograms and peak areas of each analyte and internal standard in the detected samples were recorded. The ratio of vitamin K1 to the peak area of the corresponding internal standard in the sample was calculated. The concentration of vitamin K1 in the sample could be calculated by plotting a standard curve and fitting a linear equation.

Statistical analysis

All data analyses were performed using GraphPad Prism 8 software by investigators blinded to the group allocation. Results were expressed as the mean ± SD. Statistical analysis was performed using a two-tailed Student t-test or one-way ANOVA. The measurement data had a non-normal distribution, and the non-parametric test was used. $P < 0.05$ was considered statistically significant.

Results

Characteristics of sepsis-sensitive and resistant mice

In the first study, a mouse model of inflammation was established by injection of LPS, and the survival rate of mice was observed. The timepoints for collecting donor mouse faeces are shown in Figure 1A. The susceptibility of mice to LPS-induced inflammation significantly differed. If the mice showed a moribund state within 24 h and the severity of sepsis is severe, the mice are sacrificed and defined as the S-sen group. However, the mice that survived for 7 days and recovered to the active state were identified as S-res group (Figure 1B).

Measurements of grip strength and CMAP were performed on mice in the S-sen group within 24 h when they exhibited a moribund state and sepsis severity was assessed as severe, subsequently mice were sacrificed to collect GA muscle for TUNEL staining. However, in S-res mice, mouse grip strength and CMAP were measured at day 7, subsequently mice were sacrificed to collect GA muscle for TUNEL staining. The sepsis severity scores in both groups of mice are shown in Figure 1C. The sepsis severity scores in the S-sen group were significantly higher than in the S-res group ($P < 0.05$). Apoptosis was involved in skeletal muscle atrophy.[22] Accordingly, TUNEL staining was applied to identify the apoptotic nuclei in myofibers. The number of TUNEL-positive nuclei per section in the S-sen group showed a significant increase compared with that in the S-res group ($P < 0.05$, Figure 1D). Next, we measured the body weight of the mice before sacrifice, and it was revealed that the weight of the S-sen group mice decreased markedly compared with the S-res group mice ($P < 0.01$, Figure S1A). Grip strength and EMG of the sciatic nerve-gastrocnemius complex were performed before sacrifice to explore the changes in muscle strength and evaluate neuromuscular function. The result of the grip strength measurement is presented in Figure 1E. The grip force was lower in S-sen mice than in S-res mice ($P < 0.05$). Besides, CMAP measurements are shown in Figure 1F. Amplitude and latency are depicted by measuring the distance between the dotted lines. The S-sen group also demonstrated a significant increase in CMAP latency and a significant decrease in amplitude compared with the S-res group. Abnormalities in CMAP latency and amplitude usually suggest abnormalities in the functional state of the neuromuscular junction.

Faecal bacteria transplantation from sepsis-resistant mice alleviates lipopolysaccharide-triggered muscle damage and intestinal barrier disruption

FMT trial was performed to further elucidate that the gut microbiota plays an essential part in the susceptibility of LPS-induced inflammation (Figure 2A). According to the sepsis severity score before sacrifice, the Sen group exhibited much more severe sepsis ($P < 0.05$, Figure 2B). Then, H&E staining of GA was further performed, and the size of muscle fibres was observed (Figure 2C). The GA muscle fibre diameter and CSA of the Sen group were significantly smaller than those of the Res group ($P < 0.05$, Figure 2C). Next, the effect of FMT on muscle function was assessed. The Sen mice had significantly lower grip strength than the Res mice ($P < 0.05$, Figure S1C). As shown in Figure 2D, the primary result was the Sen and Res groups replicated a phenotype similar to the donor mice, with greatly increased latency and decreased amplitude in Sen mice compared with Res mice ($P < 0.05$). Increased muscle protein breakdown due to sepsis stimulated the expression of muscle-specific E3 ubiquitin ligases MuRF-1 and MAFbx. Western blot results revealed

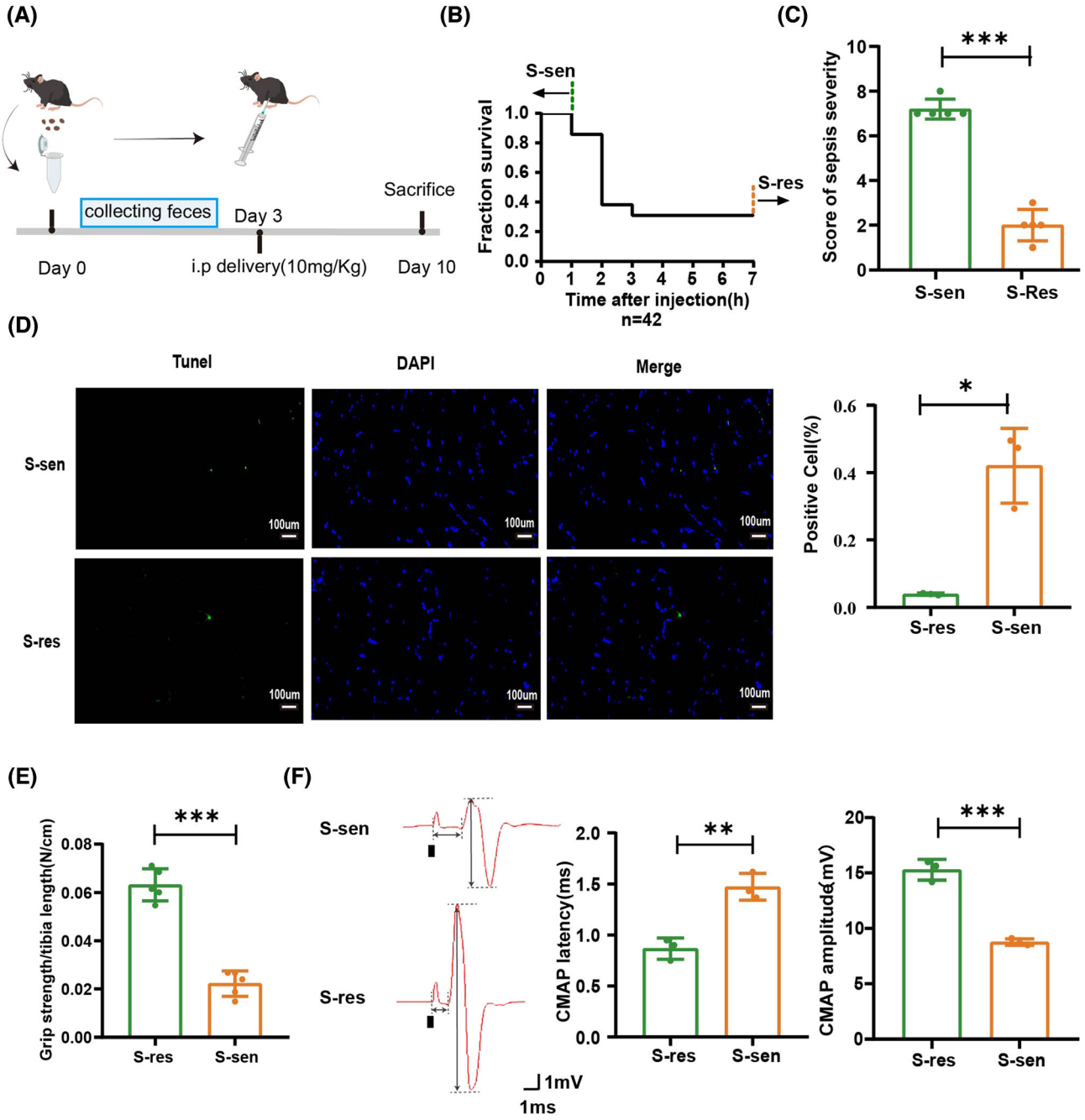

Figure 1 Characteristics of sepsis-sensitive and resistant mice. Mice were selected for intraperitoneal injection of LPS (10 mg/kg) to screen mice for susceptibility to sepsis. We defined the mice that died within 24 h as the S-sen group, whereas mice that survived for 7 days were defined as the S-res group. (A) Description of the timeline for collection of donor mouse faeces. (B) Survival was monitored for 7 days. Kaplan–Meier log-rank test was performed. S-sen n = 6/42, S-res n = 13/42. (C) The score for severity of sepsis in S-sen and S-res. (D) TUNEL staining and quantification of S-sen and S-ren GA muscle at 10× magnifications are shown (scale bars represent 100 μm). Green fluorescence represents positive cells. (E) Comparison of grip strength of S-sen and S-res. (F) Samples of CMAP recorded in S-sen and S-res. The black marks represent a single stimulus. Comparison of amplitude and latency of CMAP in S-sen and S-res in the sciatic nerve -gastrocnemius. Data are means ± SEM. P values determined through Student's t test. S-sen versus S-res: $^{*}P < 0.05$, $^{**}P < 0.01$, $^{***}P < 0.001$.

that the expression of MuRF-1 and MAFbx significantly increased in the Sen group ($P < 0.05$, Figure 2E). For further characterization of the effect of LPS on the intestinal barrier homeostasis in both groups of mice, mice colon tissues were collected for the measurement of the tight junction proteins ZO-1 and occludin. The relative expression of ZO-1 and occludin significantly decreased in the Sen mice ($P < 0.05$, Figure 2F).

DOI: 10.1002/jcsm.13379

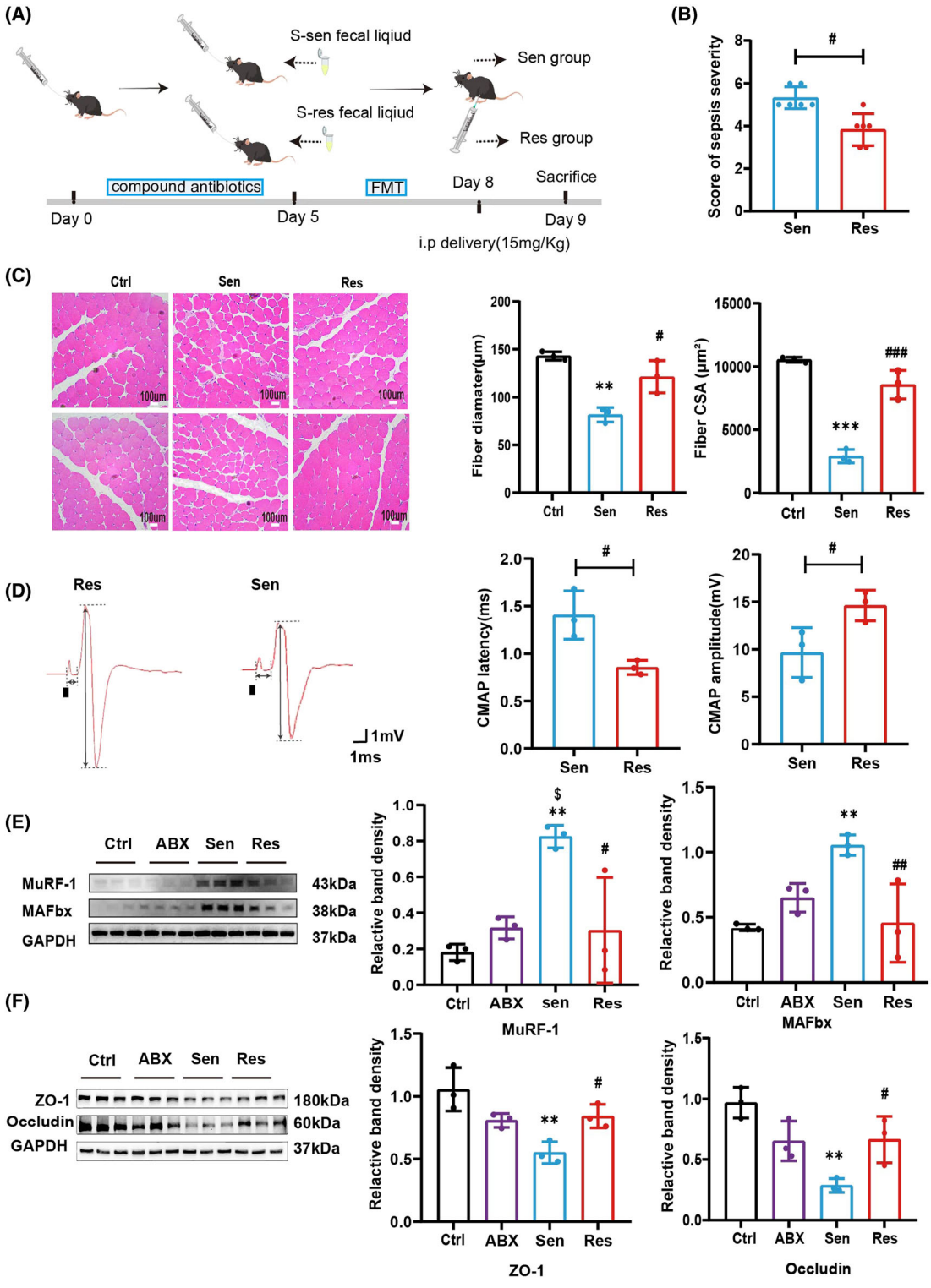

Figure 2 Faecal bacteria transplantation from S-res mice alleviates LPS-triggered muscle damage and intestinal barrier disruption. (A) Description of the steps of FMT experiment. (B) The score for Severity of sepsis in Sen and Res. (C) H&E staining in the GA muscle. Representative histological images on day 9 postoperatively (400× magnification). Scale bar = 100 μm. Comparison of muscle fibre diameter and CSA of muscle fibre in mice from each group. (D) Western blot analysis of MuRF-1 and MAFbx protein levels in TA tissue in Sen and Res groups. The results were normalized to the expression of GAPDH. (E) Western blot analysis of ZO-1 and occludin protein levels in colon tissue in Sen and Res groups. The results were normalized to the expression of GAPDH. Data are means ± SEM. *P* values determined through Student's *t* test and ordinary one-way ANOVA. Sen versus Res: $^{\#}P < 0.05$, $^{\#\#}P < 0.01$, $^{\#\#\#}P < 0.001$. Sen and Res versus Ctrl: $^{**}P < 0.01$, $^{***}P < 0.001$. Sen versus ABX: $^{\$}P < 0.05$.

DOI: 10.1002/jcsm.13379

Faecal bacteria transplantation replicates the gut microbiota composition of donor mice revealed by 16sDNA sequencing technology

Faeces from S-res and S-sen mice before LPS injection were collected as donor mouse faeces and faeces from Sen and Res mice before LPS injection were collected as recipient mouse faeces for 16SDNA sequencing to analyse the composition of the gut microbiota of donor and recipient mice. No significant differences were observed in Chao1, observed_species and shannon index between S-sen and S-res, or between Sen and Sen mice ($P > 0.05$, Figure 3A,B). The samples were constructed based on the OUT abundance-weighted unifrac distance and subjected to principal coordinate analysis, and the combination of principal coordinates with the largest contribution was selected to draw a two-dimensional Principal coordinate analysis (PCoA) plot, which shows that the two groups of samples are not clearly distinguished from each other ($P > 0.05$, Figure 3C). At the phylum level, similar gut microbiota composition can be observed in donor and recipient mice (Figure 3D).

Differences in gut microbiota composition in recipient mice revealed by 16sDNA sequencing technology

Given that the gut microbiota may be an important mediator of susceptibility to sepsis-induced muscle weakness, the changes in gut microbiota composition were explored by analysing 16SrDNA. The 16SrDNA sequencing showed that FMT treatment did not cause significant differences in α diversity between Sen mice and Res mice ($P > 0.05$, Figure 4A). PCoA results also indicated that the overall structural differences between the two groups of gut microbiota were not statistically significant ($P > 0.05$, Figure 4B). Linear discriminant effect size (LefSe) analysis was directly performed to identify simultaneous difference in the analysis of all classification levels and major bacterial biomarkers. The LDA analysis showed that Ackermanniaceae, Verrucomicrobiales, Akkermansia, Verrucomicrobiae, and Verrucomicrobiata phyla were enriched in the Sen group, and Enterococcus and Enterococcaceae were enriched in the Res group (LDA score > 4, Figure 4D). PICRUSt2 was used for metagenomic function prediction on the basis of marker genes to further explore the difference in intestinal microbial metabolic function between the two groups of mice. In accordance with the functional annotations and abundance information of the samples in the database, the top 35 functions in terms of abundance and their abundance information in each sample were selected to draw heatmaps and clustered at different functional levels. Significant functional differences were observed between the two groups of mice (Figure S2A).

Differences in gut microbiota composition in recipient mice revealed by metabolomic analysis

Considering the possible differences in gut microbial metabolic functions of Res and Sen mice, a nontargeted metabolic analysis was performed. Partial least square-discriminant analysis (PLS-DA) is a statistical method of supervised discriminant analysis using partial least square regression to model the relationship between metabolite expression and sample categories. PLS-DA demonstrated a clear separation of metabolic profiles in the Res and Sen groups (Figure 5A). Furthermore, ranking validation was performed between the two groups to determine whether the model was overfitted, and the results showed that it was not (Figure 5B). The screening of differential metabolites primarily referred to three parameters: VIP, FC, and *P*-value. The threshold values were set as VIP > 1.0, FC > 1.2 or FC < 0.833, and *P*-value < 0.05, and then 178 differential metabolites, including 90 upregulated metabolites and 88 downregulated ones in the Res group, were screened in comparison with those in the Sen group (Figure 5C). Among them, vitamin K1 (*FC* = 2.12; *P* = 0.02; *VIP* = 1.6), taurine (*FC* = 1.72; *P* = 0.03; *VIP* = 1.5) and gamma-Tocopherol (*FC* = 2.19; *P* = 0.04; *VIP* = 1.5) were significantly up-regulated in the Res group compared with the Sen group (Figures 5D and S2A,B). Subsequently, Kyoto Encyclopedia of Genes and Genomes (KEGG) analysis was used to further understand the relevant biological mechanisms. Aminoacyl-tRNA biosynthesis, ubiquinone and other terpenoid-quinone biosynthesis, and metabolic pathways were significantly enriched in the Res group compared with the Sen group (Figure 5E). For further validation, serum from the Sen and Res mice was collected before modelling, and quantitative analysis of vitamin K1 was performed using UPLC-MS/MS. Standard curves were plotted using calibrators ($r \geq 0.9500$, Figure S2D). The amount of vitamin K1 in mouse serum was determined (Figure S2E). Significantly higher levels of vitamin K1 were found in the serum of Res mice than in the serum of Sen mice (Figure S2F).

Vitamin K1 attenuates lipopolysaccharide-induced muscle damage and impaired gut barrier

Metabonomic analysis revealed that vitamin K1 was significantly enriched in the Res group. Therefore, whether vitamin K1 could ameliorate LPS-induced muscle damage and impaired intestinal barrier was determined. Mice were treated with intraperitoneal injection of LPS to induce acute inflammation model, followed by vitamin K1 gavage (Figure 6A). Sepsis severity scores were obtained, and the results showed that vitamin K1 treatment attenuated sepsis severity ($P < 0.05$, Figure 6B). After 24 h of modelling, grasp-force measurements were performed to assess muscle strength in mice. The grip strength of mice was also measured before

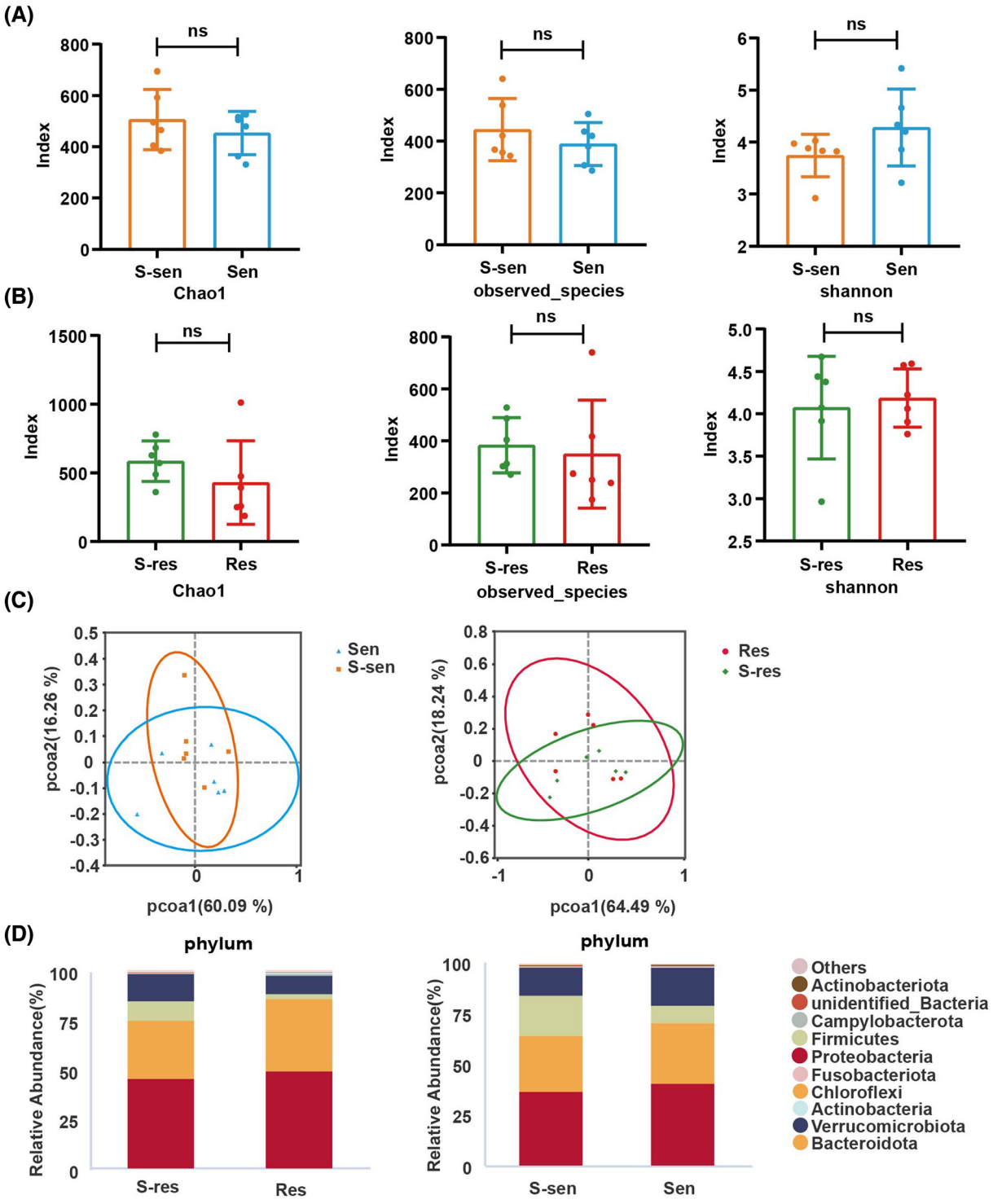

Figure 3 Faecal bacteria transplantation replicates the gut microbiota composition of donor mice. (A) Alpha Diversity Index of S-sen and Sen. The Chao1 index and observed-OTUs were calculated to estimate community richness. The shannon index was calculated to estimate community diversity. (B) Alpha Diversity Index of S-res AND Res. (C) PCoA operational taxonomic units (OTUs) based on unweighted and weighted UniFrac analyses and simulation analyses between the S-sen and Ses groups and between the S-res and Res groups. Comparison of the samples showed no significant separation between the two groups representing S-sen and Sen and between S-res and Res. S-sen group, *n* = 6; S-res group, *n* = 8; Sen group, *n* = 6; res group, *n* = 6. (D) Histogram of relative abundance of species in mice faeces at the phylum level.

DOI: 10.1002/jcsm.13379

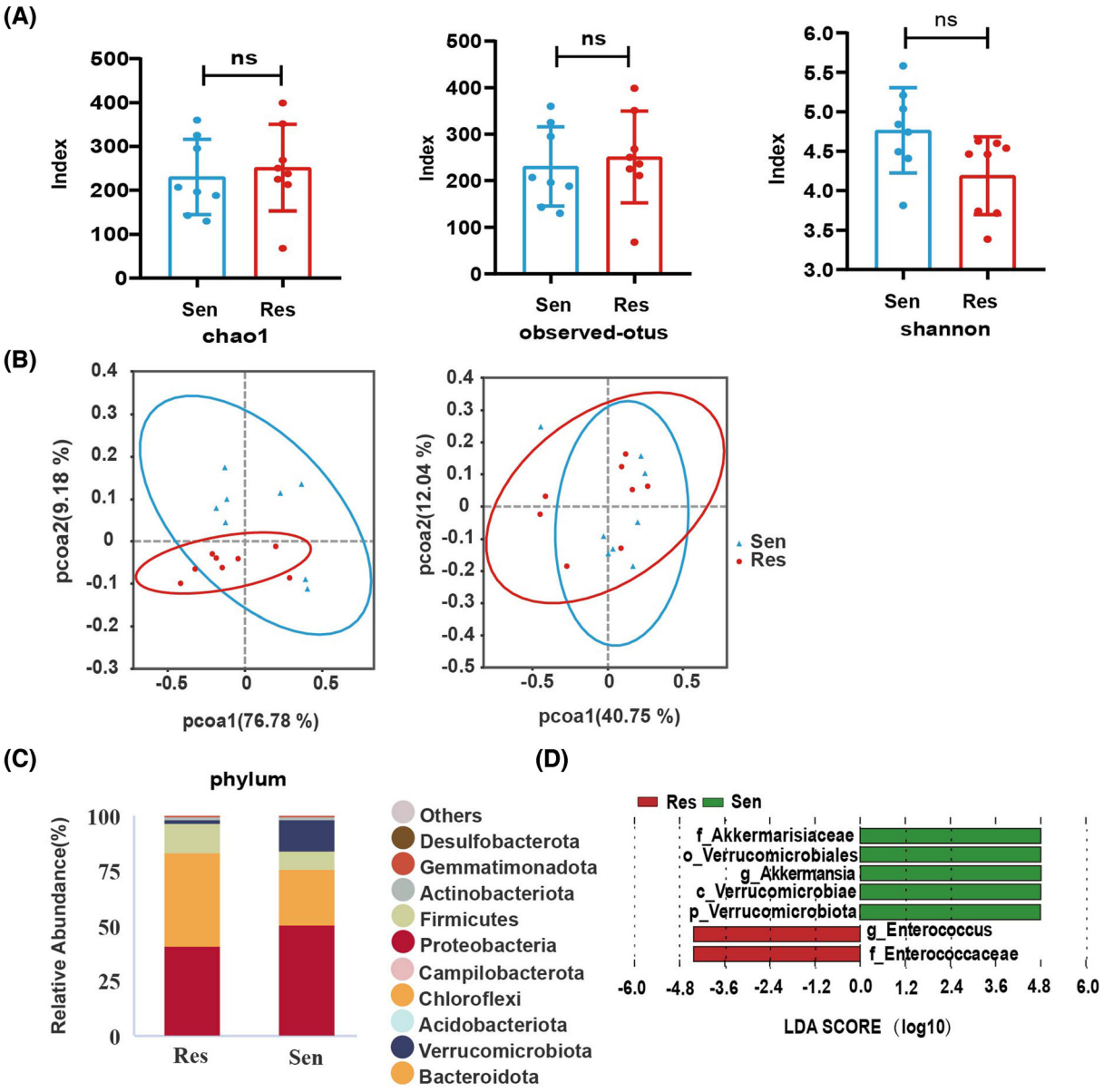

Figure 4 Differences in gut microbiota composition in recipient mice revealed by 16sDNA sequencing technology. Faeces were collected before intraperitoneal injection of LPS. (A) Alpha diversity index of Sen and Res. (B) PCoA. Comparison results of the samples revealed a unclear separation between the two clusters representing the Sen and Sen. Sen group, n = 8; res group, n = 8. (C) Histogram of relative abundance of species in mice faeces at the phylum level. (D) Histogram of the distribution of LDA values. The relative abundances of two taxa were increased, while five were decreased in the Res group compared with the Sen group.

sacrificing, and the results suggested that the grip strength of the VK1 group was significantly higher than that of the LPS group ($P < 0.05$, Figure 6C). Similarly, EMG measurements of the sciatic nerve-gastrocnemius complex revealed that pretreatment with vitamin K1 decreased latency and increased amplitude ($P < 0.05$, Figure S1E,F). Next, the expression levels of MuRF-1 and Mafbx were assessed, and the results found that treatment with vitamin K1 inhibited their expression ($P < 0.05$, Figure 6D). The ZO-1 and occludin protein expression levels were also examined to observe the effect of vitamin K1 on the functional barrier of the intestine. Sepsis disrupted the functional intestinal barrier and increased permeability. However, vitamin K1 could significantly improve it ($P < 0.05$, Figure 6E). The decline in SIRT1 was associated with increased oxidative and stress and inflammation, and SIRT1 could inhibit NF-κB-induced inflammation and downstream inflammatory cytokine synthesis.[23] Compared with the SIRT1 protein level in LPS mice, that in VK1 mice was significantly upregulated, whereas pNF-κB protein was significantly downregulated ($P < 0.05$, Figure 6F).

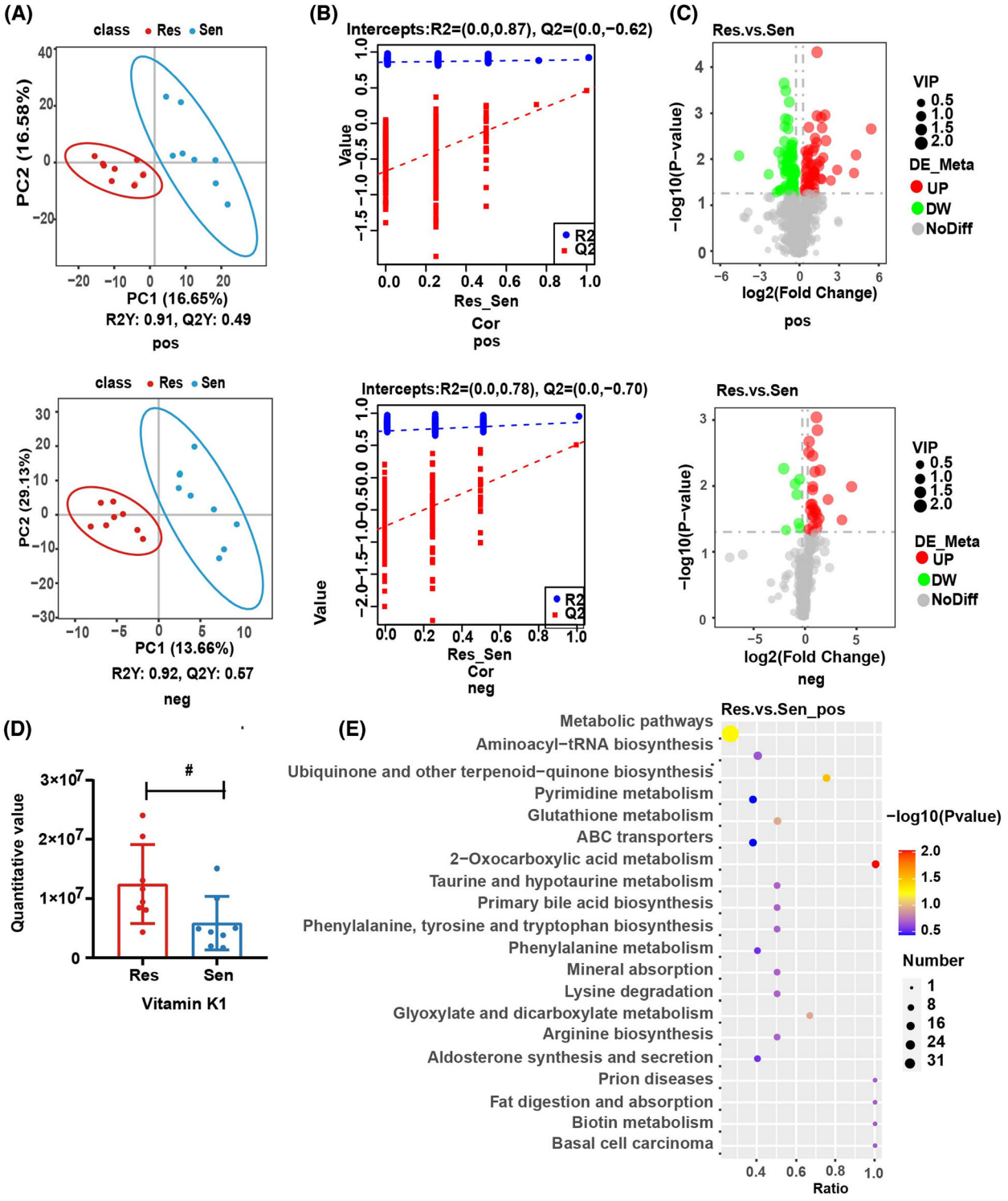

Figure 5 Differences in gut microbiota composition in recipient mice revealed by metabolomic analysis. Non-targeted metabolomics. (A) PLS-DA score scatter plot. R2Y indicates the explanatory rate of the model, Q2Y is used to evaluate the predictive ability of the PLS-DA model, and when R2Y is higher than Q2Y indicates that the model is well established. Pos means positive ions, and neg means negative ions. (B) PLSDA sequencing verification chart. When R2 is greater than Q2 and the intercept of the Q2 regression line on the Y-axis is less than zero, it indicates that the model is not 'overfitted'. (C) Volcano plots of metabolites. Each dot represents a metabolite, significantly up-regulated metabolites are represented by red dots, significantly down-regulated metabolites are represented by green dots, and the size of the dots represents the VIP value. (D) Vitamin K1 levels in faeces (nontargeted) from Sen and Res mice. (E) KEGG enrichment analysis of differential metabolites. The colour of the dots represents the P-value of the hypergeometric test, and the size of the dots represents the number of differential metabolites in the corresponding pathway.

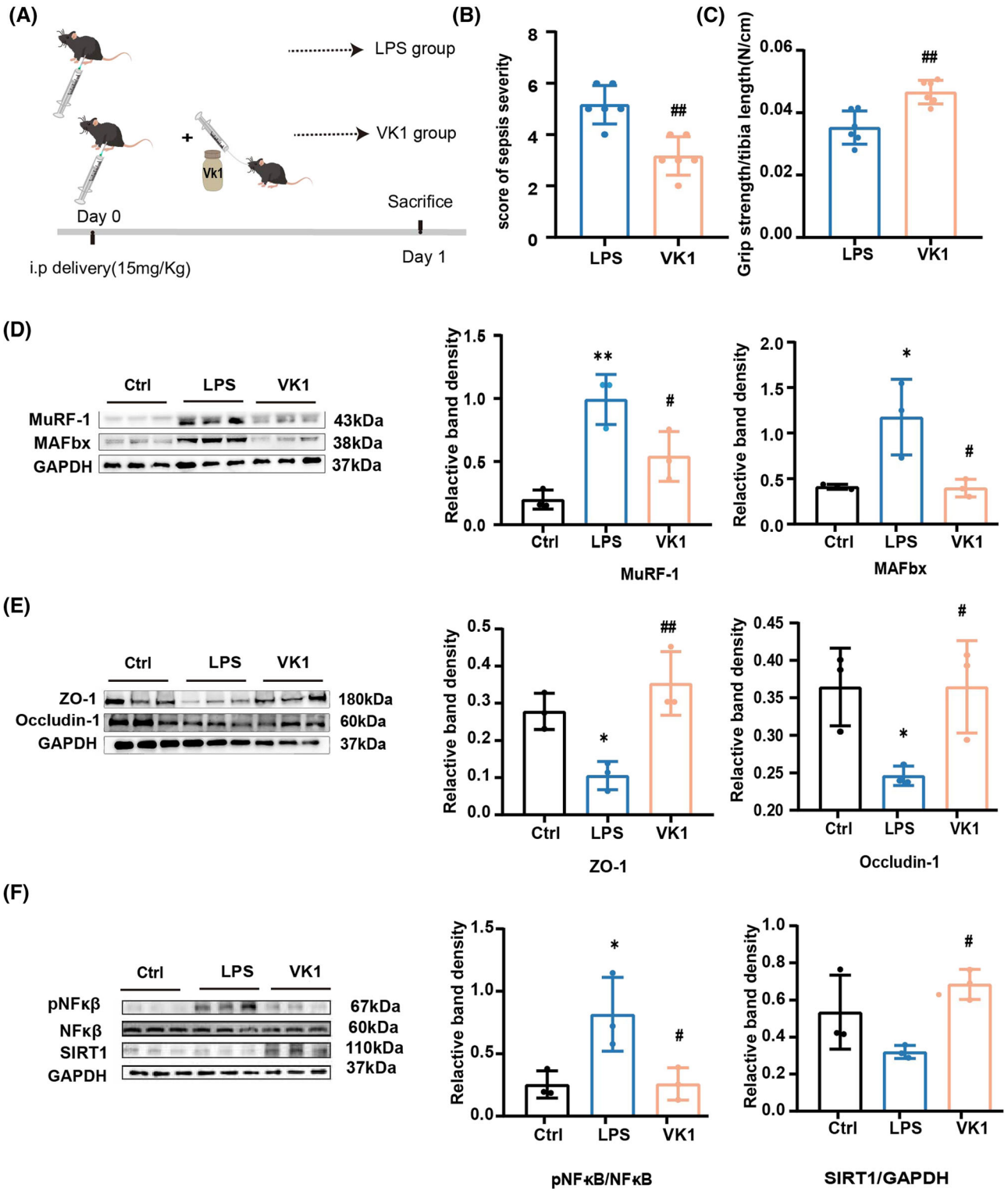

Figure 6 Vitamin K1 attenuates LPS-induced muscle damage and impaired gut barrier. (A) Description of vitamin k1 treatment experiments in mice. (B) The score for severity of sepsis in LPS and VK1. (C) Comparison of grip strength of LPS and VK1. (D) Western blot analysis of MuRF-1 and Mafbx protein levels in TA tissue in LPS and VK1 groups. The results were normalized to the expression of GAPDH. (E) Western blot analysis of ZO-1 and occludin protein levels in colon tissue in LPS and VK1 groups. The results were normalized to the expression of GAPDH. (F) Western blot analysis of SIRT1 and pNF-κB protein levels in TA muscle TAin Sen and Res groups. Data are means ± SEM. *P* values determined through Student's *t* test and ordinary one-way ANOVA. LPS versus VK1: $^{\#}P < 0.05$, $^{\#\#}P < 0.001$. LPS versus Ctrl: $^{*}P < 0.05$, $^{**}P < 0.01$.

DOI: 10.1002/jcsm.13379

Phosphoinositide 3-kinase (PI3K)/Akt/mammalian target of rapamycin (mTOR) signalling is the central pathway controlling cell growth, proliferation and metabolism. Muscle growth or atrophy is closely related to the activity of PI3K/AKT/mTOR signalling pathway. In this study, the PI3K/AKT/mTOR signalling pathway was further determined (Figure 7A). The relative expression levels of PI3K, pAKT, and pmTOR proteins were significantly downregulated in the LPS group compared with the VK1 group ($P < 0.05$, Figure 7B–D). The effect of vitamin K1 treatment on the level of oxidative stress in septic mice was subsequently observed. SOD and GR were higher and MDA was lower in VK1 mice than in LPS mice ($P < 0.05$, Figure 7E). Serum inflammatory cytokines reflect the state of inflammatory response. Significantly lower levels of inflammatory factors (IL-1 and IL-6) and TNF-α were detected in Res mice than in Sen mice ($P < 0.05$, Figure 7F).

Discussion

Gut microbiota dysbiosis reportedly plays a significant role in sepsis. Moreover, microorganisms and their metabolites are involved in multiple convergent pathways to regulate the growth and function of the host muscle.[17,24] How the gut microbiota influences skeletal muscle mass and function in sepsis remains elusive. Accordingly, this study demonstrated the role of gut microbiota and its metabolites in regulating sepsis-induced muscle weakness.

In this study, the mice of the same genetic background exhibited differences in susceptibility to LPS-induced systemic inflammation when mice inflammation models were constructed using intraperitoneal injections of LPS. This property could be replicated in other mice by FMT. The FMT assay highlighted the role of gut microbiota as an upstream susceptibility conductor of LPS-induced muscle damage. Thus, the composition of gut microbiota and metabolites in Res mice was considered to be protecting mice from sepsis. The commensal microbiome is a complex ecosystem. It varies among individuals, and it is influenced by host genotype and external environmental factors.[25,26] The 16SrDNA sequencing results suggested that the gut microbiota composition of Res and Sen mice was generally similar, although some differences in specific flora were statistically significant. The mice were purchased in the same batch and adaptively housed inside the same cage. Unlike humans, mice have coprophagy behaviour, which may result in similar gut microbiota composition.[27]

Metabolomics is closer to phenomics, which is an extension of transcriptomics and proteomics. It reflects the physiological state of an organism more directly and accurately. Metabolomics suggested that the relative content of vitamin K1 in the faeces of Res mice was significantly higher than that in the faeces of Sen mice, and serum quantification was further verified. Study 3 experiments showed that exogenous vitamin K1 administration prevented LPS-induced inflammatory response and muscle damage. Overall, these findings indicated that vitamin K1 is a potentially reliable drug for LPS-induced muscle damage treatment. A previous study reported that vitamin K1 and its derivatives could prevent lipid peroxidation and exert anti-inflammatory effects.[28,29] More importantly, vitamin K supplementation was found to reduce LPS-induced inflammation in vivo and in vitro.[30] Furthermore, vitamin K1 treatment reduced the enhanced expression of cytokine IL-6 mRNA in LPS-administered human macrophages.[31]

LPS is a major component of the outer membrane of gram-negative bacteria. In gram-negative bacterial infections, LPS is a major mediator of sepsis. LPS binding to lipopolysaccharide-binding protein (LBP) by pattern recognition receptor (PRR) can trigger the release of pro-inflammatory factors, leading to a dysregulation of the pro- and anti-inflammatory balance, which plays an important role in the development of sepsis.[32] Plasma LPS levels are commonly elevated in patients with sepsis or septic shock.[33-35] LPS-induced biological effects have been observed to be similar to those of infectious shock and is an important bacterial toxin in the pathogenesis of septic shock in humans.[36] Therefore, inhibition of LPS signalling and downstream effectors in sepsis development is a potentially promising therapeutic modality. In Study 2, we observed that after faecal microbiota transplantation, the recipient mice showed different sensitivities to LPS-induced muscle damage. LPS-induced muscle damage was mainly manifested as a decrease in mass and function. H&E staining results suggested that the size of skeletal muscle muscle fibres of the mice in the Sen group was significantly lower than that of the mice in the Res group. The results showed that the size of skeletal muscle fibres of the mice in the Res group was significantly lower than that of the mice in the Sen group. Skeletal muscle is a post mitotic tissue, and its size is mainly regulated by the protein turnover processes.[37] Studies showed that the main pathway leading to increased muscle protein catabolism under sepsis catabolism is the ubiquitin-proteasome pathway.[38] The increased expression of MuRF-1 and MAFbx in the skeletal muscle of mice in the Sen group suggested a shift in the protein homeostasis from net synthesis to net degradation in skeletal muscle, which leads to a decrease in the size of muscle fibres. Meanwhile, MuRF-1 and MAFbx protein expression levels were significantly downregulated in Res mice relative to Sen mice. The results of metabolomics analysis suggested that the levels of vitamin K1 in the faeces and serum of the Res group were significantly higher than those of mice in the Sen group. Previous studies showed that vitamin K1 could upregulate SIRT1 protein expression levels.[39]

SIRT1 is a deacetylase involved in the regulation of inflammatory response, apoptosis, and energy metabolism.[40] A key

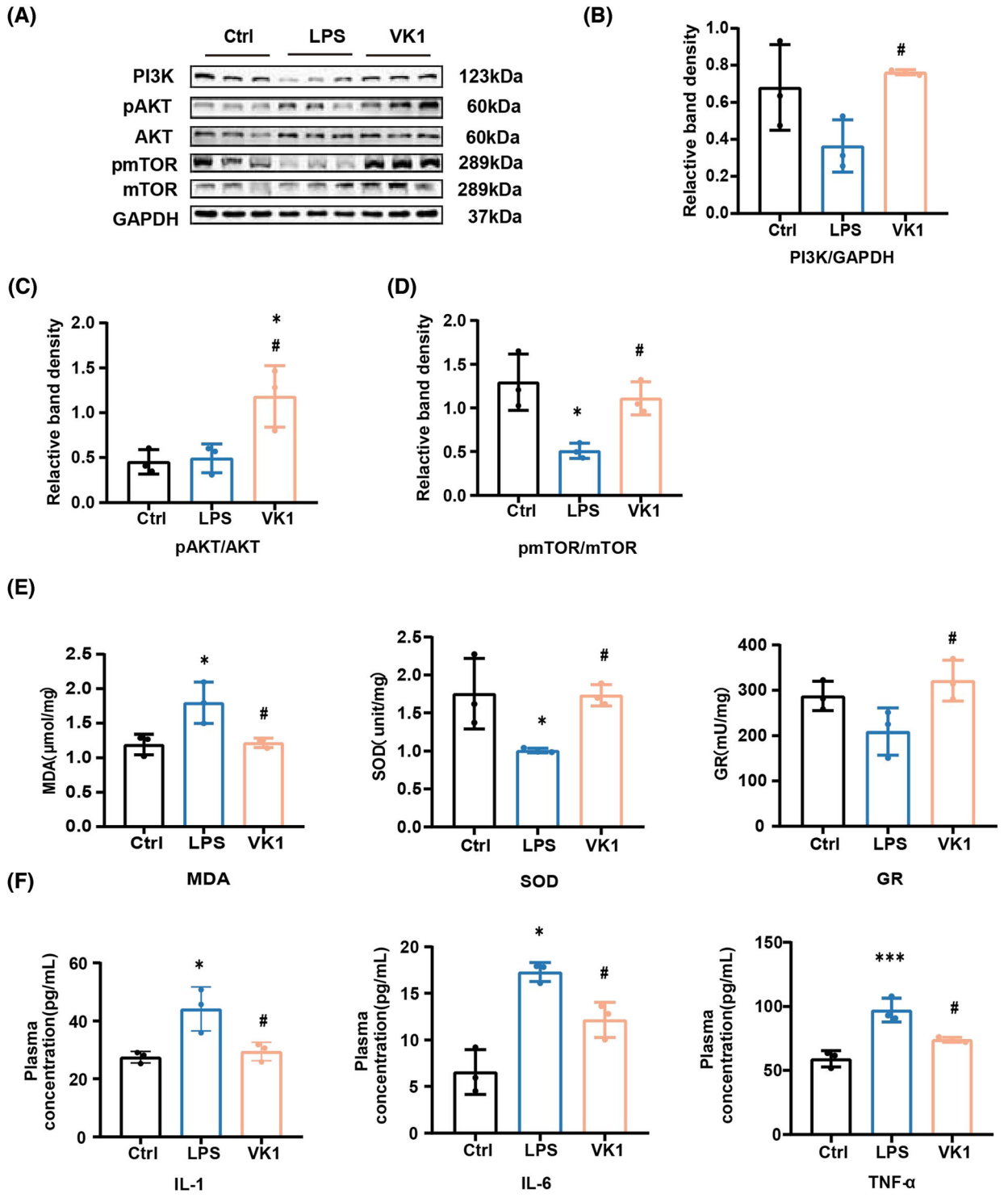

Figure 7 Vitamin K1 attenuates LPS-induced muscle damage. (A) Western blot analysis of PI3K, pAKT, AKT, pmTOR and mTOR in TA. (B)Western blot analysis of PIK3 protein levels in TA tissue in LPS and VK1 groups. The results were normalized to the expression of GAPDH. (C) Western blot analysis of pAKT protein levels in TA tissue in LPS and VK1 groups. The results were normalized to the expression of AKT. (D) Western blot analysis of pmTOR protein levels in TA tissue in LPS and VK1 groups. The results were normalized to the expression of mTOR. (E) Total SOD activity measurement, GR measurement and MDA content measurement. (F) Measurement of serum IL-1 levels, serum IL-6 levels and serum TNF-α levels. *P* values determined through ordinary one-way ANOVA. LPS versus VK1: $^{\#}P < 0.05$. LPS and VK1 versus Ctrl: $^{*}P < 0.05$, $^{***}P < 0.001$.

role for SIRT1 in balancing the immune-metabolic processes associated with acute systemic inflammation was also identified.[41] SIRT1 can antagonize NF-κB-induced inflammation. NF-κB is a key switch of the inflammatory response.[40] LPS-induced NF-κB activation plays an important role in the process of skeletal muscle atrophy.[42] In skeletal muscle, studies demonstrated that LPS could upregulate the expression of MuRF-1 and MAFbx by increasing NF-κB activity.[43,44] The significant up-regulation of SIRT1 expression and the reduced level of NF-κB protein activation in VK1 mice in the present study suggest that vitamin K1 may ameliorate LPS-induced muscle injury by down-regulating MuRF-1 and MAFbx expression mediated through SIRT1/NF-κB pathway. NF-κB activation is not only involved in protein degradation, its activation also plays an important role in inflammation.[45] Activated NF-κB induces the expression of multiple cytokines. The expression levels of inflammatory factors in the Sen group were significantly upregulated compared with those in the Res group. After vitamin K1 intervention was performed, the GR and SOD levels were significantly upregulated, whereas the MDA levels were significantly downregulated, suggesting an inhibitory effect of vitamin K1 on oxidative stress levels. Oxidative stress is characterized by an excess production of reactive oxygen species and relative nitrogen species, which could lead to inflammatory response and organ damage (Figure 8).[46,47]

The results of nontargeted metabolic analysis showed that the aminoacyl-tRNA biosynthesis is among the top pathway in the KEGG analysis. Aminoacyl-tRNA synthetases are an essential family of enzymes that play a key role in protein synthesis.[48] In non-dividing muscle cells, the PI3K/AKT/mTOR signalling pathway stimulates protein synthesis and inhibits protein degradation. This can determine muscle atrophy or growth.[49] This is consistent with previous findings that sepsis and the associated inflammatory damage produced by endotoxin (LPS) inhibit factors involved in cap-dependent

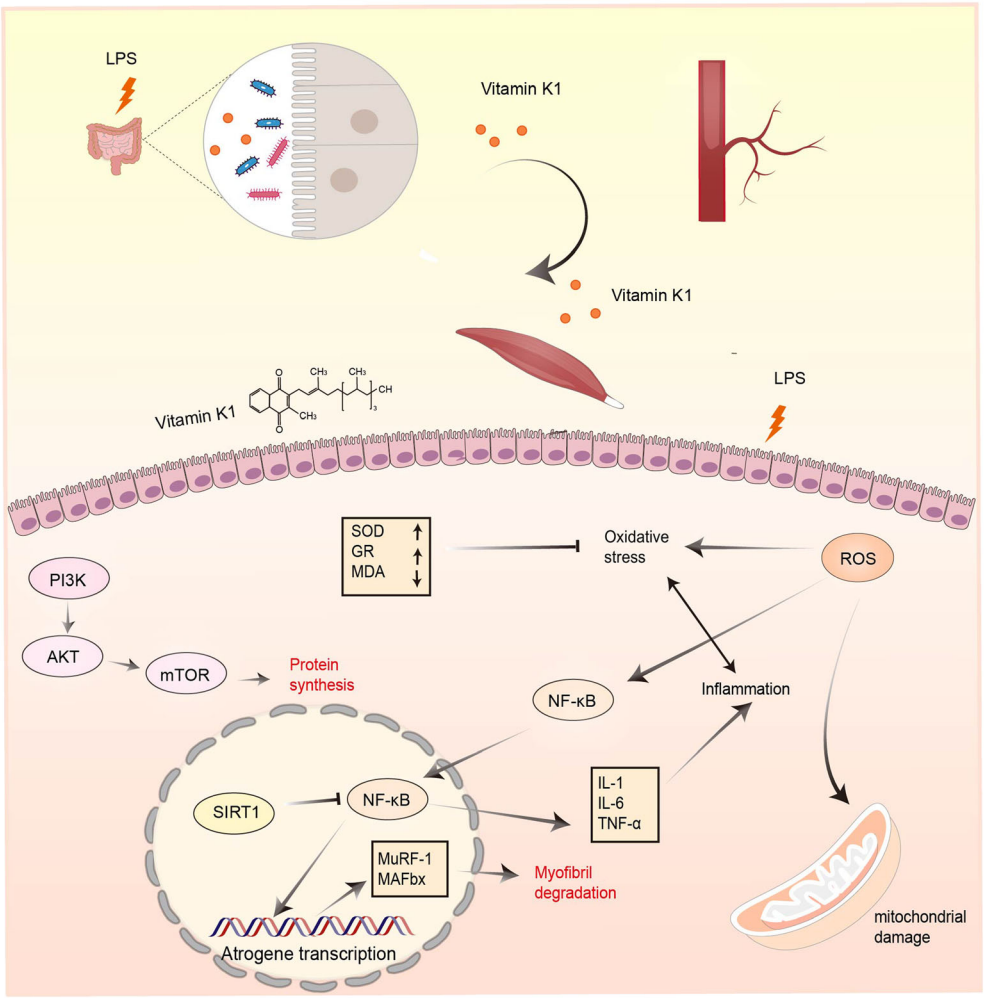

Figure 8 Working model of this work vitamin K1 might increase protein synthesis and inhibit degradation to ameliorate lipopolysaccharide-triggered muscle damage by up-regulating SIRT1 protein expression and antagonizing NF-κB activation, inhibiting LPS-induced inflammation and oxidative stress levels in skeletal muscle.

translation, namely mTOR, to suppress muscle protein synthesis. Moreover, it has been shown that sepsis does not alter the number of ribosomes, suggesting impairment of translation initiation and efficiency, as an increase in the number of free ribosomal subunits can be observed.[50] The inhibition of mTOR kinase activity is partly due to the overproduction of proinflammatory cytokines, and specific inhibitors of these cytokines restore muscle protein synthesis.[51,52] The significant decrease in the levels of skeletal muscle inflammatory factors and the significant upregulation of the PI3K/AKT/mTOR pathway after vitamin K1 intervention also suggests that the amelioration of LPS-induced muscle damage by vitamin K1 may be due, in part, to the suppression of the levels of skeletal muscle inflammation, which overcame the LPS-induced inhibition of the PI3K/AKT/mTOR pathway and restored skeletal muscle protein synthesis (Figure 8). In the present study, treatment with vitamin K1 resulted in a strong suppression of inflammation levels and a balance of redox levels, which indirectly reduced muscle atrophy and protected the functional intestinal barrier. Previous studies reported that sepsis could lead to significant mitochondrial abnormalities resulting in impaired muscle function.[53] SIRT1 could notably improve mitochondrial oxidative metabolism and regulate mitochondrial function under oxidative stress.[54] Overall, these findings indicated that vitamin K1 is a potentially reliable drug for treating sepsis-induced muscle weakness.

Our study has some limitations. Firstly, our study focused on the effect of vitamin K1 on LPS-triggered skeletal muscle damage and did not further analysis other differential metabolites and underlying mechanism. This is the next research we will continue to explore. Secondly, male mice were chosen for study in our study because it has long been noted that the inflammatory response in females differs significantly from that in males, in part related to oestrogen. This enhanced inflammatory response facilitates response to infection and sepsis, but is detrimental to the immune response against self,[55] leading to an overall higher rate of autoimmune disease in females than in males. In female inflammation, our findings have some limitations.

Conclusions

In summary, the findings suggest that intestinal metabolites are involved in sepsis-associated muscle weakness in mice. Vitamin K1 might have a protective effect against LPS-triggered muscle damage by up-regulating SIRT1, antagonizing NF-κB-activated inflammatory responses and regulating oxidative stress, promoting protein synthesis and inhibiting protein degradation. This study reveals a novel mechanism of sepsis-associated muscle weakness and suggests that vitamin K1 might be an effective strategy to prevent sepsis-associated muscle weakness.

Acknowledgements

We thank the Cardiovascular and Metabolic Laboratory of Southwest Medical University for providing the experimental platform. The authors of this manuscript certify that they comply with the ethical guidelines for authorship and publishing in the *Journal of Cachexia, Sarcopenia and Muscle*.

Conflict of interest

All authors declare that they have no conflict of interest.

Funding

This study was supported by the Sichuan Provincial Science and Technology Plan Joint Innovation Projects (No. 2022YFS0632).

Online supplementary material

Additional supporting information may be found online in the Supporting Information section at the end of the article.

References

1. Fan E, Cheek F, Chlan L, Gosselink R, Hart N, Herridge MS, et al. An official American Thoracic Society Clinical Practice guideline: the diagnosis of intensive care unit-acquired weakness in adults. *Am J Respir Crit Care Med* 2014;**190**:1437–1446.
2. Witteveen E, Wieske L, Manders E, Verhamme C, Ottenheijm CAC, Schultz MJ, et al. Muscle weakness in a *S. pneumoniae* sepsis mouse model. *Ann Transl Med* 2019;**7**:9.
3. Fletcher SN, Kennedy DD, Ghosh IR, Misra VP, Kiff K, Coakley JH, et al. Persistent neuromuscular and neurophysiologic abnormalities in long-term survivors of prolonged critical illness. *Crit Care Med* 2003;**31**:1012–1016.
4. Iwashyna TJ, Ely EW, Smith DM, Langa KM. Long-term cognitive impairment and functional disability among survivors of severe sepsis. *JAMA* 2010;**304**:1787–1794.
5. Wollersheim T, Woehlecke J, Krebs M, Hamati J, Lodka D, Luther-Schroeder A, et al. Dynamics of myosin degradation in intensive care unit-acquired weakness during severe critical illness. *Intensive Care Med* 2014;**40**:528–538.
6. Puthucheary ZA, Rawal J, McPhail M, Connolly B, Ratnayake G, Chan P, et al. Acute skeletal muscle wasting in critical illness. *JAMA* 2013;**310**:1591–1600.

7. Gong S, Yan Z, Liu Z, Niu M, Fang H, Li N, et al. Intestinal microbiota mediates the susceptibility to polymicrobial sepsis-induced liver injury by granisetron generation in mice. *Hepatology* 2019;**69**: 1751–1767.
8. Kang L, Li P, Wang D, Wang T, Hao D, Qu X. Alterations in intestinal microbiota diversity, composition, and function in patients with sarcopenia. *Sci Rep* 2021;**11**:4628.
9. Qiu Y, Yu J, Li Y, Yang F, Yu H, Xue M, et al. Depletion of gut microbiota induces skeletal muscle atrophy by FXR-FGF15/19 signalling. *Ann Med* 2021;**53**:508–522.
10. Picca A, Ponziani FR, Calvani R, Marini F, Biancolillo A, Coelho-Júnior HJ, et al. Gut microbial, inflammatory and metabolic signatures in older people with physical frailty and sarcopenia: results from the BIOSPHERE study. *Nutrients* 2019;**12**:65.
11. Lahiri S, Kim H, Garcia-Perez I, Reza MM, Martin KA, Kundu P, et al. The gut microbiota influences skeletal muscle mass and function in mice. *Sci Transl Med* 2019;**11**: 11.
12. Yan H, Diao H, Xiao Y, Li W, Yu B, He J, et al. Gut microbiota can transfer fiber characteristics and lipid metabolic profiles of skeletal muscle from pigs to germ-free mice. *Sci Rep* 2016;**6**:31786.
13. Tang G, du Y, Guan H, Jia J, Zhu N, Shi Y, et al. Butyrate ameliorates skeletal muscle atrophy in diabetic nephropathy by enhancing gut barrier function and FFA2-mediated PI3K/Akt/mTOR signals. *Br J Pharmacol* 2022;**179**:159–178.
14. Du L, Qi R, Wang J, Liu Z, Wu Z. Indole-3-propionic acid, a functional metabolite of Clostridium sporogenes, promotes muscle tissue development and reduces muscle cell inflammation. *Int J Mol Sci* 2021; **22**:12435.
15. Honda K, Littman DR. The microbiota in adaptive immune homeostasis and disease. *Nature* 2016;**535**:75–84.
16. Gong S, Lan T, Zeng L, Luo H, Yang X, Li N, et al. Gut microbiota mediates diurnal variation of acetaminophen induced acute liver injury in mice. *J Hepatol* 2018;**69**: 51–59.
17. Gai X, Wang H, Li Y, Zhao H, He C, Wang Z, et al. Fecal Microbiota transplantation protects the intestinal mucosal barrier by reconstructing the gut microbiota in a murine model of sepsis. *Front Cell Infect Microbiol* 2021;**11**:736204.
18. Wang Z, Klipfell E, Bennett BJ, Koeth R, Levison BS, DuGar B, et al. Gut flora metabolism of phosphatidylcholine promotes cardiovascular disease. *Nature* 2011;**472**: 57–63.
19. Gregory JC, Buffa JA, Org E, Wang Z, Levison BS, Zhu W, et al. Transmission of atherosclerosis susceptibility with gut microbial transplantation. *J Biol Chem* 2015; **290**:5647–5660.
20. Oliveira TS, Santos AT, Andrade CBV, Silva JD, Blanco N, Rocha NN, et al. Sepsis disrupts mitochondrial function and diaphragm morphology. *Front Physiol* 2021; **12**:704044.
21. In vivo electrophysiological measurement of the rat ulnar nerve with axonal excitability testing. United States; 2018. https://doi.org/10.3791/56102
22. Bloemberg D, Quadrilatero J. Autophagy, apoptosis, and mitochondria: molecular integration and physiological relevance in skeletal muscle. *Am J Physiol Cell Physiol* 2019;**317**:C111–C130.
23. Kumar J, Haldar C, Verma R. Melatonin ameliorates LPS-induced testicular nitro-oxidative stress (iNOS/TNFα) and inflammation (NF-kB/COX-2) via modulation of SIRT-1. *Reprod Sci* 2021;**28**:3417–3430.
24. Liang H, Song H, Zhang X, Song G, Wang Y, Ding X, et al. Metformin attenuated sepsis-related liver injury by modulating gut microbiota. *Emerg Microbes Infect* 2022;**11**:815–828.
25. Neumann M, Steimle A, Grant ET, Wolter M, Parrish A, Willieme S, et al. Deprivation of dietary fiber in specific-pathogen-free mice promotes susceptibility to the intestinal mucosal pathogen *Citrobacter rodentium*. *Gut Microbes* 2021; **13**:1966263.
26. Fassarella M, Blaak EE, Penders J, Nauta A, Smidt H, Zoetendal EG. Gut microbiome stability and resilience: elucidating the response to perturbations in order to modulate gut health. *Gut* 2021;**70**:595–605.
27. Bo T-B, Zhang X-Y, Kohl KD, Wen J, Tian S-J, Wang D-H. Coprophagy prevention alters microbiome, metabolism, neurochemistry, and cognitive behavior in a small mammal. *ISME J* 2020;**14**:2625–2645.
28. Zheng X, Hou Y, He H, Chen Y, Zhou R, Wang X, et al. Synthetic vitamin K analogs inhibit inflammation by targeting the NLRP3 inflammasome. *Cell Mol Immunol* 2021;**18**:2422–2430.
29. Kolbrink B, von Samson-Himmelstjerna FA, Messtorff ML, Riebeling T, Nische R, Schmitz J, et al. Vitamin K1 inhibits ferroptosis and counteracts a detrimental effect of phenprocoumon in experimental acute kidney injury. *Cell Mol Life Sci* 2022; **79**:387.
30. Kieronska-Rudek A, Kij A, Kaczara P, Tworzydlo A, Napiorkowski M, Sidoryk K, et al. Exogenous vitamins K exert anti-inflammatory effects dissociated from their role as substrates for synthesis of endogenous MK-4 in murine macrophages cell line. *Cell* 2021;**10**:1571.
31. Ohsaki Y, Shirakawa H, Hiwatashi K, Furukawa Y, Mizutani T, Komai M. Vitamin K suppresses lipopolysaccharide-induced inflammation in the rat. *Biosci Biotechnol Biochem* 2006;**70**:926–932.
32. Poltorak A, He X, Smirnova I, Liu MY, van Huffel C, du X, et al. Defective LPS signaling in C3H/HeJ and C57BL/10ScCr mice: mutations in Tlr4 gene. *Science* 1998;**282**: 2085–2088.
33. MacFie J, O'Boyle C, Mitchell CJ, Buckley PM, Johnstone D, Sudworth P. Gut origin of sepsis: a prospective study investigating associations between bacterial translocation, gastric microflora, and septic morbidity. *Gut* 1999;**45**:223–228.
34. Opal SM, Scannon PJ, Vincent JL, White M, Carroll SF, Palardy JE, et al. Relationship between plasma levels of lipopolysaccharide (LPS) and LPS-binding protein in patients with severe sepsis and septic shock. *J Infect Dis* 1999;**180**:1584–1589.
35. Ono Y, Maejima Y, Saito M, Sakamoto K, Horita S, Shimomura K, et al. TAK-242, a specific inhibitor of Toll-like receptor 4 signalling, prevents endotoxemia-induced skeletal muscle wasting in mice. *Sci Rep* 2020;**10**:694.
36. Parrillo JE, Parker MM, Natanson C, Suffredini AF, Danner RL, Cunnion RE, et al. Septic shock in humans. Advances in the understanding of pathogenesis, cardiovascular dysfunction, and therapy. *Ann Intern Med* 1990;**113**:227–242.
37. Rom O, Reznick AZ. The role of E3 ubiquitin-ligases MuRF-1 and MAFbx in loss of skeletal muscle mass. *Free Radic Biol Med* 2016;**98**:218–230.
38. Bodine SC, Baehr LM. Skeletal muscle atrophy and the E3 ubiquitin ligases MuRF1 and MAFbx/atrogin-1. *Am J Physiol Endocrinol Metab* 2014;**307**:E469–E484.